[8]Na. T. Y. and Turski, C. E., "Solution of the Non-Linear Differential Equations for Finite Bending of a Thin-Walled Tube by Parametric Differentiation," *Aeronautical Quarterly*, Vol. 25, Part 1, Feb. 1974, pp. 14-18.

Flow-Establishment Times for Blunt Bodies in an Expansion Tube

Charles G. Miller* and John A. Moore*
NASA Langley Research Center, Hampton, Va.

Nomenclature

M = Mach number
p_s = model surface pressure, kN/m^2
$\dot{q}_s$ = model surface heat transfer rate, MW/m^2
r_b = model base radius, cm
r_n = sphere nose radius, cm
t = time after arrival of incident shock in acceleration gas, μs
t^* = time required for shock standoff distance to obtain a steady-state value, μs
δ = shock standoff distance as function of time, cm
Δ = steady-state shock standoff distance, cm
ϵ = normal shock density ratio
τ = time interval between incident shock in acceleration gas and the interface, μs

Subscripts
5 = test gas freestream conditions
20 = acceleration gas freestream conditions

Introduction

DUE to the relatively short test-flow duration of the Langley expansion tube (approximately 100-300 μs), the time required to establish quasi-steady flow about a test model is an important consideration in data analysis. The expansion tube operating sequence differs from other hypersonic-hypervelocity impulse facilities since the test model is subjected to the acceleration gas flow prior to the test gas flow. Although results from studies of flow establishment times for blunt bodies in shock tubes (see Refs. 1-5) provide a guide, they are not directly applicable to the expansion tube. The purpose of this Note is to present flow establishment results as inferred from shock standoff distance, pressure, and heat transfer measurements in the Langley expansion tube. These experimental results were obtained as spinoff from various studies using helium, air, and CO_2 test gases at freestream velocities from 5-7 km/sec, and are preliminary to a more comprehensive study.

Apparatus and Tests

The expansion tube is basically a shock tube with a section of constant-cross-section tube attached to the downstream end. A weak, low-pressure (secondary) diaphragm separates this section, denoted as the acceleration section, from the driven section of the shock tube, which is commonly referred to as the intermediate section of the expansion tube. The intermediate section and acceleration section are evacuated and filled with the desired test gas and acceleration gas, respectively. For a given test, the acceleration gas was the same as the test gas, only at a much lower quiescent pressure. Upon rupture of the primary diaphragm in the shock-tube portion of the facility, the quiescent test gas is processed by the resulting incident shock wave. This shock-heated test-gas flow encounters and ruptures the secondary diaphragm, thereby generating an incident shock in the quiescent acceleration gas. The test gas undergoes an unsteady expansion in the acceleration section; hence, a model positioned at the exit of the acceleration section is subjected first to the incident shock in the acceleration gas and then to the shock-heated acceleration gas prior to the test gas flow. A more detailed description of the Langley 6-in.-diam expansion tube in presented in Ref. 6, along with the test-section flow conditions for the three test gases used in this study.

Shock standoff distance, δ was obtained using a single-pass Z-shaped schlieren system. Two recording systems were used simultaneously. One used a Xenon arc lamp as a light source and a high-speed framing camera to record the images. Camera speeds for the present study provided nominal time intervals between successive frames of 6.9 or 10.4 μs. This system was alined slightly off-axis and mirrors were used to prevent interference with the other system. The second system used a point light source, having a duration of approximately 150 *ns*, in conjunction with a still camera. The spark source for the still camera was alined on axis to yield the accuracy required for shock shape measurements.[6]

Model surface pressure p_s was measured using miniature piezoelectric (quartz) transducers in conjunction with charge amplifiers. These transducers were exposed to the model surface through a hole having a 1.6 mm diam and drilled at any angle so as to shield the sensing surface of the transducer from solid contaminants in the post-test flow.

Model-surface heat-transfer rates $\dot{q}_s$ were obtained using thin-film resistance gages having Pyrex 7740 substrates, platinum sensing elements, and silicone monoxide insulating films. These gages were mounted flush with the model surface and in the stagnation region. Convective heat transfer rate was determined using the voltage change of the sensing element during the test period as input to the computational method of Ref. 7.

Models tested were flat-faced cylinders and a sphere. The radius of the flat-faced cylinders r_b was varied from 0.95-3.81 cm, and the radius of the sphere r_n was 3.18 cm. Models were positioned at the acceleration section exit and tested in the open jet at zero angle of attack.

Results and Discussion

Measured normalized shock standoff distance for flat-faced cylinders of various radii and a sphere are shown in Fig. 1 as a function of test time t. Test gases are air (Fig. 1 a) and CO_2 (FIG. 1 b) at freestream Mach numbers, M_5 of 7.7 and 9.2, and normal shock density ratios, ϵ of 11.1 and 18.8, respectively. Establishing a zero time t from the film strip was not possible; hence, the first frame indicating flow about the model was assumed to correspond to a time equal to half the time interval between successive frames. Poor shock resolution of enlargements of each film frame and off-axis alinement prohibit accurate determination of shock standoff distance δ; however, the time history of δ is believed to be reasonably accurate. For a given test, values of δ for the flat-faced cylinder models were adjusted (up to 25%) to improve agreement between these values at times corresponding to essentially constant δ with the quasi-steady shock standoff distance, Δ obtained with the still camera at time t equal to 140-180 μs. Also shown in Fig. 1 are predicted[8,9] Δ for the acceleration gas flow and test gas flow. The time interval between arrival of the incident shock and the interface was inferred previously[6] to be 25-30 μs for air and CO_2.

The flat-faced cylinder results for air show a monotonic increase in δ/r_b to an essentially constant value for the three smaller radii; for the largest radius, δ/r_b initially increases, then decreases and finally increases to a nearly constant value. Similar trends are observed for CO_2. Thus, an effect of r_b on the variation of δ/r_b with t exists for the present air and CO_2 conditions. For air, the shock established symmetrically about

Received May 23, 1975; revision received July 14, 1975.
Index categories: Nonsteady Aerodynamics; Supersonic and Hypersonic Flow.

*Aero-Space Engineer, Entry Gas Dynamics Group, Advanced Entry Analysis Branch, Space Systems Division. Member AIAA.

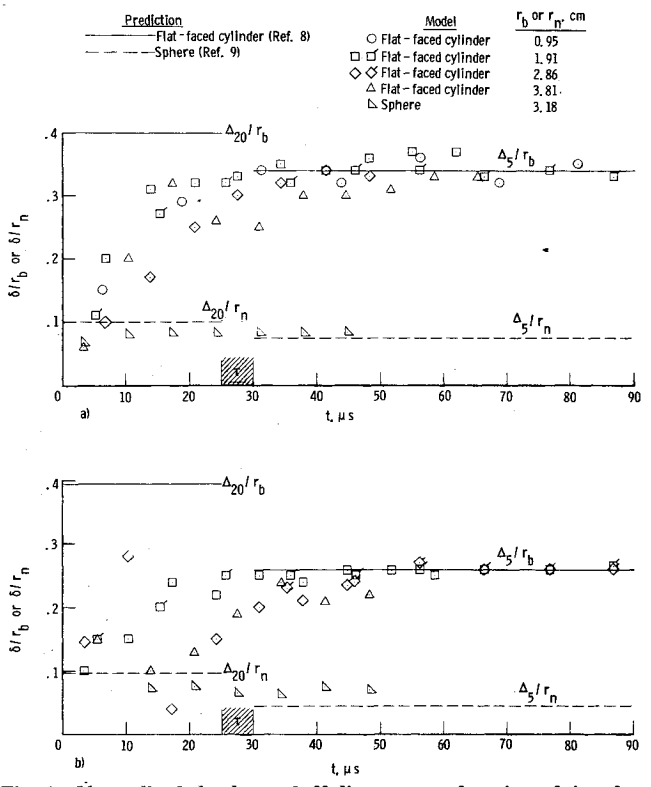

Fig. 1 Normalized shock standoff distance as a function of time for air and CO_2. a) Air; $M_5 = 7.7$, $\epsilon = 11.1$; b) CO_2; $M_5 = 9.2$, $\epsilon = 18.8$.

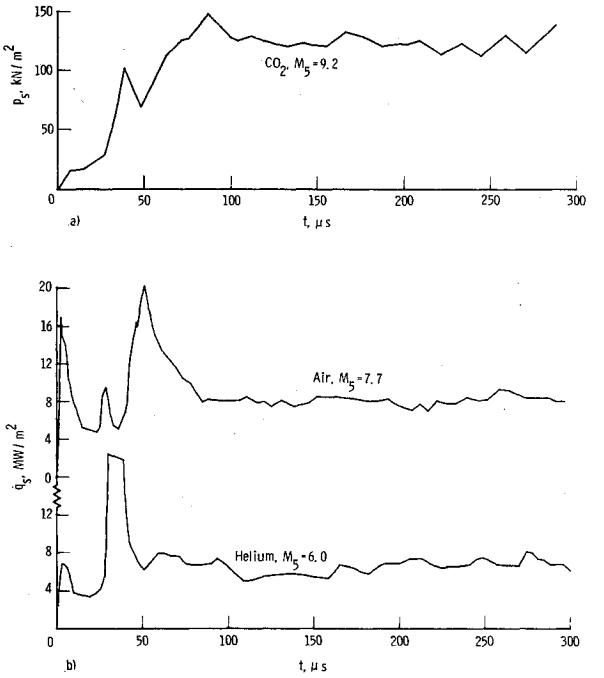

Fig. 2 Surface pressure and heat transfer rate as a function of time for a flat-faced cylinder with $r_b = 2.86$ cm. a) Stagnation-point pressure; b) Heat-transfer rate.

the flat-faced cylinder model for the two smaller radii; however, a complex, asymmetric shock existed about the models having radii of 2.86 and 3.81 cm for roughly the first 35 μs and 55 μs, respectively. An asymmetric shock development was also observed for the larger r_b of the CO_2 tests. For all tests with the flat-faced cylinder models, an essentially steady, symmetric shock existed for t greater than 60 μs, or so. Hence, the time required for flow establishment at these conditions represents less than 25% of the 250 μs test period.[6] The time required for δ/r_n for the sphere to obtain a near constant value is roughly ⅓ that for a flat-faced cylinder of the same radius. The more rapid flow establishment time for a sphere is expected in view of the results of Refs. 3, 10, and 11, which may be combined to show the ratio of establishment time (defined as the time required for δ to equal 0.98 Δ) for a flat-faced cylinder to that for a sphere is approximately equal to $0.77\sqrt{\epsilon - 1}\ (r_b/r_n)$. Shock establishment about the sphere was symmetrical for both air and CO_2.

Predicted establishment times from empirical[3] and theoretical[12] results indicate a quasi-steady value of δ for air should be obtained for the smallest r_b, and nearly obtained for r_b equal to 1.91 cm, prior to interface arrival. Similarly, prediction[2,10] for the sphere shows Δ should be achieved during the acceleration air flow. Based on these predictions, δ is expected to decrease upon interface arrival, since Δ_{20}/r_b is greater than Δ_5/r_b and Δ_{20}/r_n is greater than Δ_5/r_n. Possible nonequilibrium and viscous effects within the shock layer are expected to be more severe in the lower density acceleration flow, thereby producing a larger difference in Δ between the acceleration and test gas flows than predicted.[6] However, no detectable decrease in δ is observed for air, nor for CO_2 and these same models, upon interface arrival. The present time histories of δ do not appear to provide a means for determining the time of interface arrival, τ.

Variation of stagnation-point surface pressure p_s with time for a flat-faced cylinder is shown in Fig. 2 a for CO_2 test gas. Response of the pressure instrumentation is good (less than 5 μs, or so) as indicated by the initial pressure increase corresponding to incident shock arrival. This pressure history indicates that the time interval τ is approximately 25-30 μs, and the p_s becomes constant (within $\pm 20\%$) with time roughly 70 μs after incident shock arrival. Similar flat-faced cylinder pressure histories obtained for air test gas also yield establishment times for p_s somewhat larger than inferred from measured δ; however, experimental uncertainties preclude any conclusion concerning these relatively small differences in inferred establishment time. Predictions[10] for a sphere indicate the p_s approaches its steady-state value more readily than δ, but as noted in Ref. 10, pressure histories for a sphere may be significantly different than for a flat-nosed body.

Shown in Fig. 2 b is the stagnation-region surface heat transfer rate $\dot{q}_s$ as a function of time for a flat-faced cylinder with rounded corner (corner radius equal to 0.5 body radius) in air flow, and sharp corner in helium flow. (Rounding the corner is expected to reduce the flow establishment time somewhat, since the flat-faced cylinder becomes more sphere-like.) The time interval τ is difficult to define from the thin-film voltage output for air, but appears to be between 25-40 μs. The $\dot{q}_s$ is essentially constant for times greater than 80 μs, thereby representing a 20-30 μs increase over the time required to establish a quasi-steady value of δ. This result may be because δ is primarily an indicator of the time required for the inviscid flowfield to establish, whereas heat transfer rate depends on the establishment of the viscous layer as well.

The time required for $\dot{q}_s$ to reach a quasi-steady value for helium was less than that for air, even though the flat-faced cylinder model tested in helium had a sharp corner. Time of arrival of the interface is well defined by the thin-film output voltage and is equal to 30 μs. Establishment time of $\dot{q}_s$ for helium was approximately 50 μs, and thus implies establishment time for $\dot{q}_s$ decreases with increasing specific heat ratio. This trend, but for δ, is predicted [10] for a sphere for the present test gases.

In conclusion, time histories of shock detachment distance illustrate the shock formation about the smaller-radii flat-faced cylinders and the sphere was symmetrical, whereas a complex, asymmetric formation was observed for the larger-radii cylinders. These measurements also showed the flow established more readily about the sphere than a flat-faced cylinder of the same diameter. Model surface pressure and

heat transfer rate time histories provide information on the time of arrival of the acceleration gas-test gas interface, whereas shock standoff distance time histories do not. This implies the shock standoff distance is not as sensitive to change in flow conditions as pressure and heat transfer rate for these expansion tube tests. Heat transfer results revealed flow establishment for helium test gas is more rapid than for air test gas. The present measurements demonstrate that quasi-steady flow exists about relatively large, blunt models during two-thirds of the approximate 250 μs expansion tube test period.

References

[1]Offenhartz, E. and Weisblatt, H, "Determination of the Time History of the Flow Field About Blunt Bodies in a Shock Tube," RAD-TR-2-58-4 (Contract No. AF-04 (645)-30), May, 1958, AVCO.

[2]Syshchikova, M.P., Berezkina, M.K., and Semenov, A.N., "Formation of Frontal Shock Waves at Blunt Bodies in Shock Tubes," *Soviet Physics-Technical Physics*, Vol. 9., No. 11, May 1965, pp. 1549-1553.

[3]Davies, L. "Bow-Shock Establishment and Stagnation-Point Pressure Measurements for a Blunt-Nosed Body at Supersonic Speeds,", Aeronautical Research Council, Current Paper 776, 1965, Her Majesty's Stationary Office, London.

[4]Zienkiewicz, H.K. and Mallock, I.D., "Establishment of the Bow-Wave in the Supersonic Flow of Carbon Dioxide Past a Sphere," *Aeronautical Quarterly*, Vol. 19, Part 1, Feb. 1968, pp. 51-58.

[5]Bryson, A.E. and Gross, R.W.F., "Diffraction of Strong Shocks by Cones, Cylinders, and Spheres," *Journal of Fluid Mechanics* Vol. 10, Part 1, Feb. 1961, pp. 1-16.

[6]Miller, C.G., "Shock Shapes on Blunt Bodies in Hypersonic-Hypervelocity Helium Air and CO_2 Flows, and Calibration Results in Langley Expansion Tube," TN D-7800, 1975, NASA.

[7]Cook, W.J. "Determination of Heat-Transfer Rates From Transient Surface Temperature Measurements," *AIAA Journal*, Vol. 8, July 1970, pp. 1366-1368.

[8]South, J.C., Jr., "Calculation of Axisymmetric Supersonic Flow Past Blunt Bodies With Sonic Corners, Including a Program Description and Listing," TN D-4563, 1968, NASA.

[9]Barnwell, R.W., "A Time-Dependent Method for Calculating Supersonic Blunt-Body Flow Fields With Sharp Corners and Embedded Shock Waves," TN D-6031, 1970, NASA.

[10]Barnwell, R.W., "Numerical Results for the Diffraction of a Normal Shock Wave by a Sphere and for the Subsequent Transient Flow," TR R-268, 1967, NASA.

[11]Serbin, H., "The High Speed Flow of Gas Around Blunt Bodies," *Aeronautical Quarterly*, Vol. 9, Nov. 1958, pp. 313-330.

[12]Anderson, G.F., "Real Gas Effects on the Time Required for Establishing a Detached Bow Shock," *AIAA Journal*, Vol. 5, Feb. 1967, pp. 366-367.

Technical Comments

Comment on "A New Method of Solution of the Eigenvalue Problem for Gyroscopic Systems"

Bertrand T. Fang*
Wolf Research and Development Corporation, Riverdale, Md.

MEIROVITCH[1] considered the following eigenvalue problem governing the oscillation of gyroscopic systems

$$\lambda IX + GX = 0 \tag{1}$$

where λ is the eigenvalue, X the corresponding eigenvector, I and G are even-order real nonsingular matrices, the former symmetric and the latter skew-symmetric. By means of the nonsingular transformation $X = ABY$, with A being the orthogonal matrix which diagonalizes I, and B, the diagonal matrix which normalizes the diagonalized I, Eq. (1) is transformed to

$$\lambda B^T A^T IABY + B^T A^T GABY = \lambda Y - PY = 0 \tag{2}$$

where $P = -B^T A^T GAB$ is a skew-symmetric matrix. Thus it is seen that the eigenvalue problem considered is really equivalent to a standard eigenvalue problem for a skew-symmetric matrix P. Traditionally skew-symmetric eigenvalue problems have not been of much interest, although results such as the eigenvalues are conjugate imaginary pairs, the eigenvectors are orthogonal, etc., are reasonable well-known[2-4] Since efficient algorithms for computing the eigenvalues and eigenvectors of real symmetric matrices are available,[2,5] the skew-symmetric eigenvalue problem may be solved by noting if λ and X are eigenvalue and eigenvector of P; i.e., $PX = \lambda X$, then

$$P^2X = P(PX) = P(\lambda X) = \lambda PX = \lambda^2 X \tag{3}$$

That is, λ^2 and X are eigenvalue and eigenvector of P^2, which is a symmetric matrix. A slight complication exists because P^2 has a two-fold multiplicity of all its eigenvalues, and for each eigenvalue there exists a two-dimensional subspace in which every vector is an eigenvector. This ambiguity may be resolved by noting if X_1 and X_2 are a pair of orthonormal eigenvectors of P^2, associated with the eigenvalue λ^2, then the corresponding eigenvectors of P are $X = \alpha X_1 \pm i\alpha X_2$. Many of the results and derivations in Ref. 1 follow immediately from the previous result. It may also be pointed out that the transformation from Eqs. (14) and (17) to Eqs. (20) and (22) in Ref. 1 has been programed as Subroutine NROOT in the IBM Scientific Subroutine Package.

Received January 16, 1975; revision received March 26, 1975.
Index categories: Spacecraft Attitude Dynamics and Control; Structural Dynamic Analysis.

*Senior Scientific Specialist, Planetary Sciences Department.

References

[1]Meirovitch, L., "A New Method of Solution of the Eigenvalue Problem for Gyroscopic Systems," *AIAA Journal*, Vol. 12, Oct. 1974, pp. 1337-1342.

[2] Marcus, M., *Basic Theorems in Matrix Theory*, AMS-57, 1964, National Bureau of Standards. Washington D.C.

[3]Franklin, J.N., *Matrix Theory*, Prentice-Hall, Englewood Cliffs, N.J., 1968, p. 117.

[4]Perlis, S., *Theory of Matrices*, Addison Wesley, Reading, Mass., 1952, pp. 196-210.

[5]Subroutine EIGEN, IBM System 360 Scientific Subroutine Package, IBM Corp., White Plains, N.Y.